THE ALTERNATING TRANSMISSION LINE MATRIX (ATLM) SCHEME

P. Russer[1,2], B. Bader[1]

[1]Ferdinand-Braun-Institut für Höchstfrequenztechnik, Rudower Chaussee 5, D-12489 Berlin, Germany
[2]Institut für Hochfrequenztechnik, Technische Universität München, Arcisstr. 21, D-80333 München, Germany

ABSTRACT

A novel alternating transmission line matrix scheme (ATLM) is presented where the TLM cells are subdivided into two subsets of mutually neighbouring cells. Within each time step the state of one subset of cells is computed from the states of the neighbouring cells at the previous time step. Compared with existing TLM schemes the numerical effort as well as the storage requirements are reduced by 50% without loss of accuracy. Furthermore, spurious solutions occuring in existing TLM schemes can be avoided by ATLM.

INTRODUCTION

The TLM method has proven to be a very powerful method of electromagnetic field computation [1]. In TLM, the continuous space is discretized by introducing a TLM mesh with the TLM nodes as the elementary elements. The electromagnetic field is represented by wave pulses scattered in the nodes and propagating in transmission lines between neighbouring nodes. This picture of TLM stresses the analogy to the network concept. Originally TLM is based on the analogy between the electromagnetic field and a mesh of transmission lines [2]. The three-dimensional TLM method with symmetrical condensed node (SCN) introduced by Johns [3] has been derived directly from Maxwell's equations using the Method of Moments [4].

Comparing TLM schemes with finite difference (FD) schemes one characteristic property of all TLM schemes is that a pair of canonically conjugated E and H field components is sampled together in one space-time point. In contrast to this the classical FD schemes sample the E and H field components at different points. In Yee's so-called leapfrog FDTD scheme the sampling points for the E field components and the H field components are mutually shifted by half a discretization interval of the time coordinate as well as for the space coordinate [5].

However, compared with FD schemes all known TLM schemes suffer from a serious drawback which has not been considered in literature up to now. Considering a homogeneous domain modelled by TLM nodes without stubs the state of a TLM cell for a given discrete time coordinate only depends on the states of the neighbouring cells at the previous time coordinates. In homogeneous regions modelled by TLM without stubs there is no mutual dependence of the states of neighbouring cells. This can be seen clearly if we define a so-called parity p assigned to TLM wave pulses discrete space coordinates l, m, n and the discrete time coordinate k by

$$p = \text{sign}\,(k+l+m+n)\,. \qquad (1)$$

If the sum $k+l+m+n$ is even then $p=+1$ and if $k+l+m+n$ is odd then $p=-1$. Now it is easy to check that in any TLM mesh without stubs and boundaries the TLM pulses depend only on previous pulses with the same parity. The lack of interference between pulses with different parity has serious consequences which can easily be verified. Choosing for example different initial conditions for cells with even and odd parity will result in a parallel computation of these two problems specified for the cells with odd and even parity. You will see that the even and odd cells and their corresponding evolving field distributions change their places with each time step but both field

CH3577-4/95/0000-0019$01.00 © 1995 IEEE

distributions do not interfere. If the initial conditions are chosen with smooth distribution over the whole mesh it may happen that the field evolution is spatially smooth. However this will be in the sense of a prestabilized harmony between even and odd states and not by a causal relation. The result will not be more accurate than from computing only the evolution of the states with even parity and getting the states with odd parity at the end of the computation by interpolation. Therefore the numerical effort as well as the storage requirements may be reduced by 50% without any loss in accuracy by restricting the computation to states with only one parity. Considering for example only states with even parity means that for even k only the states of cells with even $l+m+n$ are defined and for odd k only the states of cells with odd $l+m+n$ are defined.

If we restrict the computation to pulses with one parity we have to avoid boundary conditions and stubs which link odd and even pulses. Boundaries spaced by the half discretization interval $\Delta l/2$ from the nodes as well as stubs with length $\Delta l/2$ couple pulses with even and odd parity. This coupling by perturbation cannot be considered as a remedy for the above stated problems. Therefore the solution of our problem is to avoid the coupling of pulses with different parities also at boundaries and in the case of modelling regions with different material parameters. This is achieved by avoiding transmission line elements of length $\Delta l/2$. If in the whole TLM scheme only transmission line elements of length Δl are used, the parity of all transmitted and reflected pulses is conserved. In principle all existing TLM schemes may be adapted in this way. However, stubs of length Δl as well as distances Δl between the nodes and the walls would degrade the accuracy of the TLM computation. Therefore TLM schemes which allow to model variable material parameters as for example the symmetrical supercondensed node (SSCN) proposed by Trenkic et al. [6, 7] should be preferred.

THE SSCN TLM SCHEME

The SSCN allows anisotropic media to be modelled without stubs [6, 7]. We restrict our considerations to the case of a regular orthogonal mesh with equal spatial discretization intervals Δl in all three directions. Fig. 1a shows the SSCN. The structure of the SSCN is identical with the structure of the SCN. However the $\boldsymbol{S}$-matrix of the SSCN is different from the $\boldsymbol{S}$-matrix of the SCN and is given by

$$\boldsymbol{S} = \begin{pmatrix} \boldsymbol{R}_0 & \boldsymbol{S}_0 & \boldsymbol{S}_0^T \\ \boldsymbol{S}_0^T & \boldsymbol{R}_0 & \boldsymbol{S}_0 \\ \boldsymbol{S}_0 & \boldsymbol{S}_0^T & \boldsymbol{R}_0 \end{pmatrix} \tag{2}$$

with the submatrices

$$\boldsymbol{R}_0 = \begin{pmatrix} -\rho & 0 & 0 & 0 \\ 0 & -\rho & 0 & 0 \\ 0 & 0 & \rho & 0 \\ 0 & 0 & 0 & \rho \end{pmatrix},$$

$$\boldsymbol{S}_0 = \begin{pmatrix} 0 & 0 & \tau & -\tau \\ 0 & 0 & -\tau & \tau \\ \tau & \tau & 0 & 0 \\ \tau & \tau & 0 & 0 \end{pmatrix} \tag{3}$$

and the parameters ρ and τ given by

$$\rho = \sqrt{1 - \frac{1}{\varepsilon_r}} \quad , \qquad \tau = \frac{\sqrt{1-\rho^2}}{2} \quad , \tag{4}$$

where ε_r is the relative permittivity. The relative permeability is kept $\mu_r = 1$. Note, that six of the diagonal elements of the $\boldsymbol{S}$-matrix are identical and have positive sign. The other six diagonal elements are of opposite sign. We have two groups of lines with different characteristic impedances Z_+ and Z_-. The positive reflection coefficients ρ belong to the ports with the lower characteristic impedances Z_- whereas the negative reflection coefficients belong to the ports with the higher characteristic impedances Z_+.

In [4] it is shown that for the conventional SCN TLM scheme introducing the wave amplitudes with respect to the TLM cell boundaries yields a bijective one-to-one mapping between the 24 transverse electric and magnetic field components and the 2×12 TLM wave amplitudes. In the network model of TLM, in each sampling point, one port is assigned to each polarization. By this way, we assign an elementary multiport to each TLM cell. In the literature, this multiport is called

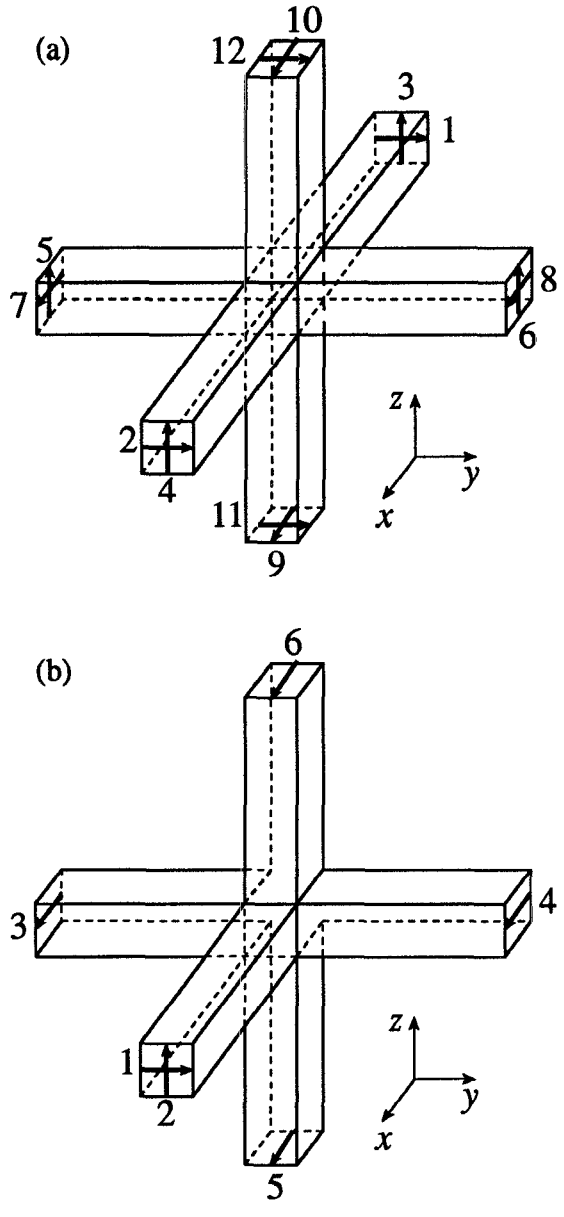

Fig. 1: (a) the symmetrical supercondensed node and (b) electric wall half-node.

the TLM node. The term TLM *cell* denotes the geometrical object we have defined in the continous space, whereas the term TLM *node* denotes the abstract network model representing the relations between the wave amplitudes in the sampling points of a TLM cell. In the ATLM scheme we have reduced the number of wave pulses by a factor of two compared with the conventional TLM scheme. This allows to sample the electric and magnetic field components in the mesh nodes and also to achieve a bijective one-to-one mapping between the electric and magnetic field components and the wave amplitudes.

MODELLING OF THE WALLS

Moving the boundaries into the TLM node planes requires the introduction of boundary and wall nodes for plane surfaces, corners and edges. Therefore ATLM requires a library for the different wall and boundary types. In the following we restrict ourselves to the consideration of the nodes describing the plane electric wall and the plane magnetic wall. For these wall types each of the wall nodes exhibits six ports. Fig. 1b shows the electric wall node. We obtain the electric wall node from the SSCN twelve-port by short-circuiting the ports 5, 6, 11, and 12 and letting the rear ports 1 and 3 unterminated. The electric wall scattering matrix $\boldsymbol{S}_{ew}$ for the remaining ports 2, 4, 7, 8, 9, and 10 is renormalized for the characteristic impedances $(Z_+, Z_-, Z_+/2, Z_-/2, Z_+/2, Z_-/2)$. With

$$\kappa = \frac{\sqrt{1-\rho^2}}{\sqrt{2}} \tag{5}$$

we obtain

$$\boldsymbol{S}_{ew} = \begin{pmatrix} -\rho & 0 & -\kappa & \kappa & 0 & 0 \\ 0 & \rho & 0 & 0 & -\kappa & \kappa \\ -\kappa & 0 & \rho & 0 & \tau & \tau \\ \kappa & 0 & 0 & \rho & \tau & \tau \\ 0 & -\kappa & \tau & \tau & -\rho & 0 \\ 0 & \kappa & \tau & \kappa & 0 & -\rho \end{pmatrix} \tag{6}$$

The ports 1 and 2 describe field components parallel to the wall, whereas the ports 3, 4, 5, and 6 describe electric field components normal to the wall and magnetic field components parallel to the wall. Considering the scattering matrix $\boldsymbol{S}_{ew}$ we see that a wave pulse with horizontal polarization incident in port 1 is not only backscattered but also scattered into ports 3 and 4 and from there backscattered via the neigbouring nodes.

We obtain the magnetic wall node from the SSCN twelve-port letting the ports 7, 8, 9, and 10 unterminated and by short-circuiting the rear

ports 1 and 3. The magnetic wall scattering matrix S_{mw} for the remaining ports 2, 4, 5, 6, 11, and 12 is renormalized for the characteristic impedances $(Z_+, Z_-, 2Z_+, 2Z_-, 2Z_+, 2Z_-)$.

$$S_{mw} = \begin{pmatrix} -\rho & 0 & 0 & 0 & \kappa & \kappa \\ 0 & \rho & \kappa & \kappa & 0 & 0 \\ 0 & \kappa & -\rho & 0 & \tau & -\tau \\ 0 & \kappa & 0 & -\rho & -\tau & \tau \\ \kappa & 0 & \tau & -\tau & \rho & 0 \\ \kappa & 0 & -\tau & \tau & 0 & \rho \end{pmatrix} \quad (7)$$

NUMERICAL EXAMPLE

As an example we modelled a via-hole on GaAs substrate as depicted in fig. 2. The substrate height is $h_s = 100\mu m$. The metallization thickness of the line is $h_l = 3\mu m$ and the diameter of the via is $d = 60\mu m$. For calculating the S-parameters of the via-hole, we considered only one half of the structure with a symmetry plane. The mesh was discretized by $65 \times 128 \times 94$ TLM nodes in cubic cells with $\Delta l = 3\mu m$.

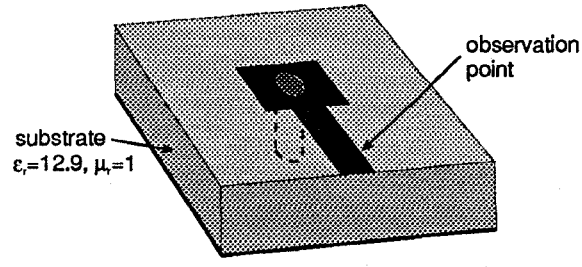

Fig. 2: Via-hole.

Fig. 3 shows the scattering parameter $|S_{11}|$ as calculated with traditional TLM and ATLM. The reduction of the computational effort and the memory requirements, both by a factor of 2, does not affect the accuracy of the computation.

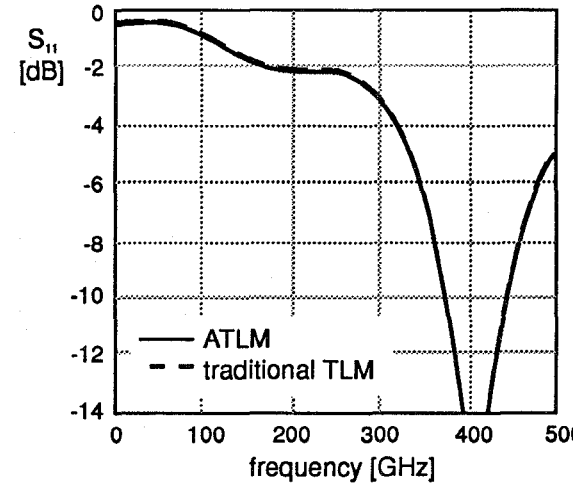

Fig. 3: Comparison of the reflexion coefficients $|S_{11}|$ simulated with ATLM and with traditional TLM.

REFERENCES

[1] W. J. R. Hoefer, "The Transmission Line Matrix (TLM) Method", Chapter 8 in "Numerical Techniques for Microwave and Millimeter Wave Passive Structures", edited by T. Itoh, J. Wiley, New York, 1989, pp. 496-591

[2] G. Kron, "Equivalent Circuit of the Field Equations of Maxwell I", Proc. IRE, vol. 32, May 1944, pp. 289-299

[3] P. B. Johns, "A Symmetrical Condensed Node for the TLM-Method", IEEE Trans. Microwave Theory Tech., vol. MTT-35, no. 4, Apr. 1987, pp. 370-377

[4] M. Krumpholz, P. Russer, "A Field Theoretical Derivation of TLM", IEEE Trans. Microwave Theory Tech., vol. MTT-42, no. 9, Sep. 1994, pp. 1660-1668

[5] K. S. Yee, "Numerical Solution of Initial Boundary Value Problems Involving Maxwell's Equations in Isotropic Media", IEEE Trans. on Antennas and Propagation, vol. AP-14, no.3, May 1966, pp. 302-307

[6] V. Trenkic, C. Christopoulos, T. M. Benson, "New Symmetrical Super-Condensed Node for the TLM Method", Electronics Letters, vol. 30, no. 4, Feb. 1994, pp. 329-330

[7] V. Trenkic, C. Christopoulos, T. M. Benson, "Generally graded TLM Mesh Using the Symmetrical Supercondensed Node", Electronics Letters, vol. 30, no. 10, May 1994, pp. 795-797